© 2001 The Chemical Society of Japan

Accounts

Theoretical and Computational Study of Thermoreversible Gelation

Fumihiko Tanaka* and Tsuyoshi Koga

Department of Polymer Chemistry, Graduate School of Engineering, Kyoto University,
and KIPS (Kyoto Institute of Polymer Science), Sakyo-ku, Kyoto 606-8501

(Received August 10, 2000)

This paper reviews recent theoretical and computational studies of thermoreversible gelation with multiple cross-link junctions in associating polymers. Paying special attention to the *multiplicity* and *sequence* length of the network junctions, we derive phase diagrams with coexisting gelation and phase separation. Local and global structures of the gel networks are studied. The conventional Eldridge–Ferry method is extended to allow for simultaneous evaluation of multiplicity and sequence length (or enthalpy of the cross-links), and applied to the experimental gel melting curves of poly(vinylalcohol) in water. On the basis of the Scanlan–Case criterion, we calculate the number of *elastically effective chains* and of *dangling ends* in the network as functions of polymer concentration and temperature. The effect of added surfactants on the formation of thermoreversible gels (*surfactant-mediated gelation*) in hydrophobically modified associating polymer solutions is also studied under the assumption of the existence of a minimum multiplicity required for stable cross-links. Competition between intramolecular micellization and intermolecular cross-linking is also studied with special attention to the formation of *flower micelles*.

In this paper, we review our recent theoretical and computational studies on thermoreversible gelation in associating polymers. An associating polymer (hereafter referred to as AP) is a polymer carrying associative groups (or segment blocks) along the backbone or on the chain side.[1] Typical model APs that have recently been the focus of study are water-soluble polymers partially modified by hydrophobic groups. One series of APs are based on poly(ethylene oxide) chains (referred to as PEO), being modified by short alkyl chains,[2–7] propyrene oxide (or butylene oxide) chains[8] and fluorocarbon chains.[9–12] Hydrophobes are either periodically or randomly attached on a polymer chain. The simplest one is a telechelic polymer carrying two hydrophobes at the chain ends. Another series of APs are based on cellulose derivatives. Some examples are ethyl hydroxyethyl cellulose (EHEC)[13–15] and hydroxypropyl methyl cellulose (HPMC).[16,17] Polyelectrolytes partially modified by hydrophobic groups have also been intensely studied.[18–22]

Associative groups form aggregates, or micelles, through hydrogen bonds, ionic attraction, hydrophobic interaction, etc. Polymers with associative interactions exhibit a variety of condensed phases, typical examples of which are microscopically ordered phases, gels, and liquid crystals.[23–28] All of these phases have their counterparts formed by covalently bonded polymers, but, since association is thermally controllable, associating phases provide a new pathway to modelling statistical clusters, block copolymers, and reversible networks. APs also exhibit characteristic rheological properties such as shear thickening[2,7,29] at relatively low shear rate, so that they imply vast industrial applications as rheology control agents.

The strength of association is described by the *association constant* defined by

$$\lambda(T) \equiv \exp(-\beta \Delta f_0), \tag{0.1}$$

where $\beta \equiv 1/k_B T$ is the reciprocal temperature, and Δf_0 the standard free energy change on binding a single associative group into an aggregate, or a network junction. If the associative group (or block) consists of ζ statistical segments, as in aggregation of hydrophobic short chains, the free energy change can be written as

$$\Delta f_0 = \zeta(\Delta h - T\Delta s) \tag{0.2}$$

by the use of the binding enthalpy Δh and entropy Δs *per statistical unit*. The number ζ is called the *sequence length* of a junction.

Another important structural parameter of a junction is its multiplicity. The multiplicity k is defined by the number of groups combined together in a single junction. A cross-link by covalent bond has multiplicity $k = 2$ because of the pairwise bonding. However, most thermoreversible gels have multiple cross-links, markedly in contrast to pairwise bonding of the chemical cross-linking.

From a dynamic point of view, the time scale of reorganization in the network junctions is characterized by the *average duration time* τ_x for an associative group to be in a bound state. It is governed by the free energy barrier $\Delta F^{\dagger}$ separating the bound state from the free one:

$$\tau_{\times} = \tau_0 \exp(\beta \Delta F^{\dagger}). \tag{0.3}$$

(τ_0 being a microscopic time of monomer motion.) The rheological time scale governing the dynamics of transient networks can therefore be adjusted by this barrier height in the associative interaction.[30,31]

1 Model Solution

1.1 Theoretical Model —Multiple Association—. We first present a theoretical description of the model AP solution. We consider a mixture of associative molecules (functional molecules in conventional terminology) in a solvent. Molecules are distinguished by the number f of the associative (functional) groups they bear, each associative group being capable of taking part in the junctions with variable multiplicity which may bind together any number k of such groups.[32,33] We include $k = 1$ representing unassociated groups. In what follows, we allow junctions of all multiplicities to coexist, in proportions determined by the thermodynamic equilibrium conditions. Let n_f be the number of the statistical segments on an f-functional molecule, and let N_f be the number of f-functional primary molecules in the solution. The weight fraction w_f of the associative groups carried by the molecules with specified f relative to the total number of associative groups is then given by

$$w_f = fN_f / \sum fN_f. \tag{1.1}$$

The number and weight average functionality of the primary molecules are then defined by

$$f_n \equiv (\sum w_f / f)^{-1}, \tag{1.2}$$

and

$$f_w \equiv \sum f w_f. \tag{1.3}$$

In thermal equilibrium, the solution has a distribution of clusters with a population distribution fixed by the equilibrium conditions. Following the notation used by Fukui and Yamabe,[32] we define a cluster of type (**j**,**l**) to consist of j_k junctions of multiplicity k (k = 1,2,3,...) and l_f molecules of functionality f (f = 1,2,3,...). The bold letters $\mathbf{j} \equiv \{j_1,j_2,j_3,...\}$ and $\mathbf{l} \equiv \{l_1,l_2,l_3,...\}$ denote the sets of indices. An isolated molecule of functionality f, for instance, is indicated by $\mathbf{j}_{0f} \equiv \{f,0,0,...\}$, and $\mathbf{l}_{0f} \equiv \{0,...,1,0,...\}$.

The multiplicity of junctions is in principle determined by the equilibrium requirement for a given associative interaction. In the case of hydrophobic interaction, the chain length of a hydrophobe, the strength of water-hydrophobe interaction, the geometric form of an aggregate, and other factors determine the association constant $\lambda(T)$ and the multiplicity of junctions. In the present theoretical study, we avoid complexity in finding the precise distribution of the multiplicity, but instead, we introduce a model junction[33] in which multiplicities lying in a certain range covering from $k = s_{\min}$ to $s_{\max}$ are equally allowed. We thus have

$$k = 1(\text{free}),\ \ k = s_{\min}, s_{\min}+1, ..., s_{\max}(\text{associated}). \tag{1.4}$$

When only a single value is allowed, i.e., $s_{\min} = s_{\max} \equiv s$, we call the model *fixed multiplicity model*. Thus, for $s = 2$, fixed multiplicity model reduces to pairwise association. Such assumption of *mini-max junction* can be to some extent justified in the molecular simulation of AP described below by using a simple attractive potential among associative groups.

To deal with concentrations, we start from the conventional lattice-theoretical picture of polymer solutions,[34–36] and choose the unit of volume to be that of a unit cell, and we make the customary simplifying assumption that the solvent molecules, the functional groups and the statistical repeat units of the primary chain molecules all occupy this same volume, a^3. This is not a serious restriction.

Thus, if $N(\mathbf{j};\mathbf{l})$ is the number of (**j**;**l**)-clusters in the system, their number density is $\nu(\mathbf{j};\mathbf{l}) = N(\mathbf{j};\mathbf{l})/\Omega$ and their volume fraction is

$$\phi(\mathbf{j};\mathbf{l}) = \left(\sum_{f\geq 1} n_f l_f\right) \nu(\mathbf{j};\mathbf{l}), \tag{1.5}$$

where Ω is the total number of lattice cells in the system. The total volume fraction of the polymer component is thus given by $\phi = \sum_{\mathbf{j},\mathbf{l}} \phi(\mathbf{j};\mathbf{l})$.

1.2 Computational Model —Periodic Associating Polymers—. In order to see how APs form clusters and networks, we perform Monte Carlo (MC) computer simulations[37] in parallel to the theoretical study described above. Here we focus on the competition between intramolecular micellization and intermolecular cross-linking. As a model chain, we employ an off-lattice bead-spring model as schematically shown in Fig. 1. Associative beads are placed periodically along the chain in every p–1 non-associative beads. The potential energy for a polymer chain with n beads consists of the following three terms:

$$H = H_b + H_\theta + H_{nb}. \tag{1.6}$$

Here, H_b is the conventional finitely extensible nonlinear elastic (FENE) potential[38]

$$H_b = -\sum_{i=1}^{n-1} \frac{k_b}{2}(l_{\max} - l_0)^2 \ln\left[1 - \left(\frac{l_i - l_0}{l_{\max} - l_0}\right)^2\right], \tag{1.7}$$

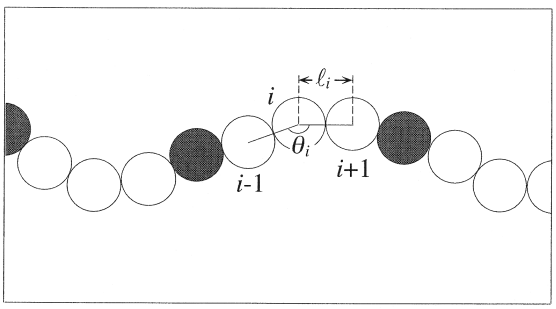

Fig. 1. Model chain employed in our MC simulation. Gray beads indicate associative groups, while white beads non-associative monomers.

to assure chain connectivity, where k_b is the spring constant, and l_i, l_0, and l_{max} are the instantaneous length of bond i, the equilibrium bond length, and the maximum bond length, respectively. The bond angle θ_i between successive bonds is kept close to the equilibrium value θ_0 by the bending potential

$$H_\theta = \sum_{i=2}^{n-1} \frac{k_\theta}{2}(\cos\theta_i - \cos\theta_0)^2. \tag{1.8}$$

Finally, H_{nb} given by

$$H_{nb} = \sum_{i<j}^{(nb)} u(r_{ij}), \tag{1.9}$$

represents interaction between the beads that are not directly connected by a spring, where u is the pair-potential, r_{ij} the distance between beads i and j, and $\sum^{(nb)}_{i<j}$ indicates summation over all distinct pairs of non-bonded beads. Excluded volume interaction with hard-sphere diameter σ is assumed to act between all pairs of non-bonded beads, while associative interaction is introduced among associative groups which attract with each other via the square-well potential

$$u(r_{ij}) = \begin{cases} \infty, & r_{ij} < \sigma \\ -\varepsilon, & \sigma \le r_{ij} < d \\ 0, & d \le r_{ij}, \end{cases} \tag{1.10}$$

Parameters in the model are chosen as follows. Length is scaled by the hard-sphere diameter σ as a unit of length. We set $l_0 = 1$ and $l_{max} = 1.2$ to avoid bond crossing, and $k_b/k_BT = 50$. Neighboring beads are on average in contact with each other in an equilibrium state because the equilibrium bond length l_0 is chosen to be equal to the hard-sphere diameter σ. Interesting results due to chain stiffness are expected to come out by adjusting the bending constant k_θ, although most of the studies presented here do not take this term into account ($k_\theta = 0$). Important dimensionless parameters in our model are the interaction range d, and the relative strength of the associative interaction ε/k_BT. In the present study, d is fixed at 1.2 and ε/k_BT is changed from 0 to 6.

In our MC simulations, we employ Metropolis algorithm.[39] A bead is chosen at random and its position is displaced by $\Delta\boldsymbol{r}$ ($|\Delta r_i| \le 0.3$, $i = x,y,z$). The energy change ΔH caused by this displacement is calculated. If $\Delta H < 0$, the new conformation is accepted; otherwise the Boltzmann factor $\exp(-\Delta H/k_BT)$ for the displacement is compared with a random number in the range [0,1]. Only if the Boltzmann factor is larger than this random number, the new conformation is accepted.

In a special case where our model AP chain consists of one associative bead only with no non-associative bead, the solution reduces to a system of hard spheres interacting via an attractive potential well. Gelation and phase separation (gas-liquid phase transition) in such interacting *sticky spheres* were studied as a model system of particulate gels.[40–42]

2 Sol/Gel Transition and Phase Separation

2.1 Theoretical Criterion of the Gel Point. We briefly summarize our lattice theory of network-forming polymer solutions.[33,43] The free energy change on passing from the standard reference state (polymers and solvent molecules being separated in hypothetical crystalline states) to the final solution, at equilibrium with respect to cluster formation, is given by the expression

$$\frac{\beta\Delta F}{\Omega} = \nu_0 \ln\phi_0 + \sum_{\mathbf{j},\mathbf{l}} \nu(\mathbf{j};\mathbf{l})[\Delta(\mathbf{j};\mathbf{l}]) + \ln\phi(\mathbf{j};\mathbf{l})] + \chi\phi_0\phi \tag{2.1}$$

in the pregel regime. The subscript zero denotes the solvent, with volume fraction $\phi_0 = 1 - \phi$. The quantity $\Delta(\mathbf{j};\mathbf{l})$ involves the free energy change accompanying the formation of a $(\mathbf{j};\mathbf{l})$-cluster in a hypothetical undiluted amorphous state from the separate primary molecules in their standard states:

$$\Delta(\mathbf{j};\mathbf{l}) \equiv \beta\left\{\mu^\circ(\mathbf{j};\mathbf{l}) - \sum_f l_f\mu^\circ(\mathbf{j}_{0f};\mathbf{l}_{0f})\right\}. \tag{2.2}$$

In the postgel regime where a cluster grows to a macroscopic network, the free energy has an additional contribution from the gel part. We leave its details to the literature.[33,43]

By minimizing this free energy with respect to the volume fraction $\phi(\mathbf{j};\mathbf{l})$, the most probable distribution of clusters is found. This process can be performed in a more systematic way by deriving chemical potentials for all types of clusters from the free energy, and imposing on them the chemical equilibrium conditions

$$\Delta\mu(\mathbf{j};\mathbf{l}) = \sum l_f\Delta\mu(\mathbf{j}_{0f};\mathbf{l}_{0f}). \tag{2.3}$$

Now the free energy $\Delta(\mathbf{j};\mathbf{l})$ consists of three parts: combinatorial, conformational, and bonding ones. The combinatorial part comes from the number of different ways to form a cluster of the type $(\mathbf{j};\mathbf{l})$ from the separate primary molecules. The conformational part comes from the change in the conformational entropy on binding each chain into a cluster, and the bonding term comes from the free energy change on binding associative groups into the junctions of specified types. To use the multiple tree statistics[32] for the combinatorial entropy of cluster formation, we assume that all clusters take tree form as in the classical literature.[44,45] Cycle formation within a cluster is neglected. We also use lattice-theoretical entropy of disorientation[34,36] for the conformational entropy. We thus find the volume fraction of clusters as a function of the temperature and concentration.

To summerize the result, we introduce the extent α of association, or conversion, that is defined by the probability for a randomly chosen associative group to be associated. It is the counterpart of the extent of reaction in conventional chemical gels. Let p_k be the probability for a randomly chosen group to be in the junction of multiplicity k. The extent α is then expressed as

$$\alpha \equiv \sum_{k\ge2} p_k. \tag{2.4}$$

Then, $p_1 \equiv 1 - \alpha$ is the probability for a hydrophobe to remain unassociated. This is equivalent to the normalization condition $\sum p_k = 1$. This condition indicates that the total concentration ψ of the hydrophobes should satisfy the relation

$$\lambda(T)\psi = zu(z), \tag{2.5}$$

where $\lambda(T)$ is the association constant given by (0.1), and the function $u(z)$ to be used to characterize junctions is defined by

$$u(z) \equiv \sum_{k=1}^{\infty} \gamma_k z^{k-1}. \tag{2.6}$$

The coefficient γ_k comes from the surface free energy of an aggregate with multiplicity k. The parameter z that appeared in the above relations is defined by $z \equiv \lambda(T)\psi p_1 = \lambda(T)\psi(1-\alpha)$, and gives the (reduced) concentration of the hydrophobes that remain unassociated in the solution.

The next step is to calculate the weight-average molecular weight of the clusters. From its divergence, we find the sol/gel transition point. It is most generally given by[32,33]

$$(f_w - 1)(\mu_w - 1) = 1, \tag{2.7}$$

where f_w defined by (1.3) is the weight average functionality of the primary chains, and $\mu_w \equiv \sum_{k \geq 1} k p_k$ the average multiplicity of the junctions. For monodisperse functionality, this equation reduces to

$$(f-1)zu'(z)/u(z) = 1. \tag{2.8}$$

For a specific model of mini-max junction (1.4), we have

$$u(z) = 1 + \sum_{k=s_{\min}}^{s_{\max}} z^{k-1} = 1 + (z^{s_{\min}-1} - z^{s_{\max}})/(1-z) \tag{2.9}$$

by neglecting possible contributions from micellar surfaces and setting all $\gamma_k = 1$ for $s_{\min} \leq k \leq s_{\max}$.

For example, the above normalization relation for the fixed multiplicity model of monodisperse polymers (f and n definite) is given by

$$\lambda(T)\phi/n = \alpha^{1/s'}/f(1-\alpha)^{s/s'}, \tag{2.10}$$

which connects the extent α of association to the (scaled) polymer concentration. From here on, abbreviations $f' \equiv f - 1$ and $s' \equiv s - 1$ are used.

The gel point condition (2.8) gives $fs'\alpha = 1$ and hence $\alpha = \alpha^* \equiv 1/f's'$ leading to the critical concentration

$$\lambda(T)\phi^*/n = f's'/f(f's' - 1)^{s/s'}, \tag{2.11}$$

where ϕ^* is the volume fraction of the polymer at gelation. As the multiplicity is changed, with other parameters kept fixed, gelation concentration changes and the sol/gel line shifts on the temperature–concentration plane.

Phase equilibria and thermodynamic stability can be studied by using chemical potentials of the polymer and of the solvent. These are derived above by differentiating the free energy. Binodal curves and spinodal curves can then be drawn on the temperature and concentration plane. In such AP solutions, gelation and phase separation generally compete with each other, and as a result phase diagrams with higher order critical points[46] such as tricritical point and critical endpoint are derived.[33,43,47]

2.2 Gel Point in Simulation. We first study conformation of a single periodic AP chain. In a simulation box, we generate a chain molecule with the degree of polymerization $n = 41$ carrying $f = 11$ stickers (period $p = 4$). We find that, for ε/k_BT larger than a certain threshold value (about 3.5 for the present molecular parameters), the stickers are strongly bonded with each other and form a single aggregate. This behavior is similar to the coil-globule transition observed in homopolymers in a solution. However, the characteristic feature of periodic APs is that the aggregates are covered by non-attractive beads, as shown in Fig. 2(a). The aggregates can therefore be regarded as microphase-separated intramolecular micelles. In Fig. 2(b), a typical snapshot obtained by the simulation for $n = 81$ and $f = 21$ is presented. With twice as large number n of statistical units, the micelle splits into two micelles of similar size. These two micelles do not merge into a single one up to at least 10^7 MC steps. We therefore consider that these intramolecular micelles are thermodynamically stable because the attractive interaction between micelle cores is screened by non-attractive coronas. We thus confirm that there is an upper bound $s_{\max}$ in the aggregation number of a micelle. This bound comes from the space-filling condition and strongly depends on the period of the stickers along the chain and the potential width $d - \sigma$. Our theoretical assumption of the maximum multiplicity is therefore justified by simulation.

The existence of the upper bound suggests that, if we use a longer polymer chain, several flower micelles are formed along the chain. In fact, experimental observation of a structure formed by a train of flower micelles along a chain was reported for amphiphilic graft copolymers in a selective solvent.[48] An example of *pearl-necklace structure* obtained in our simulation is shown in Fig. 2(c).

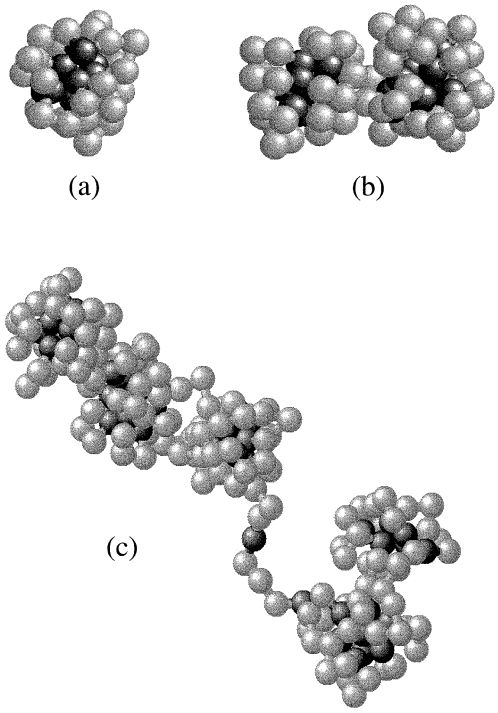

Fig. 2. at $\varepsilon/k_BT = 5$. (a) $n = 41$, a single microphase-separated micelle. (b) $n = 81$, the micelle splits into two stable ones of similar size. (c) $n = 201$, AP takes pearl-necklace structure.

From such behavior of a single chain, we expect that associative groups will form micellar cross-links between different chains. To confirm this expectation, we perform MC with two molecules. Other conditions used in the simulation are the same as those in the single chain case. A typical snapshot obtained is presented in Fig. 3. There are three aggregates in this figure; the left and the right one are intramolecular aggregates, but the one in the center is formed by the mixture of stickers belonging to different molecules. The size of the micelle is almost the same as intramolecular ones. The binding energy is $\varepsilon/k_BT = 5$. In principle, an aggregate can serve as a multiple cross-linking region if there are many chains. We therefore expect that the solution should eventually form gel with networks whose junctions are microphase-separated multichain micelles.

In a solution, many clusters are formed. Figure 4 shows a typical snapshot of MC on the telechelic polymers consisting of 7 beads at the volume fraction $\phi = 0.03$. The non-associative beads are replaced by bonds to give a clear picture. In contrast to the conventional tree assumption, many small loops are formed. The smallest loop in this solution is that formed by a single chain. Such single-chain loops, called "*petals*", attach to the junctions in clusters. Loops made up of two or three chains

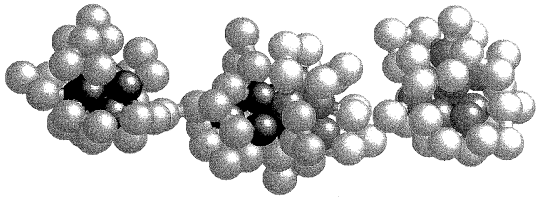

Fig. 3. An intermolecular cross-link in MC. Two chains, each carrying 61 beads, are cross-linked by forming an intermolecular micelle.

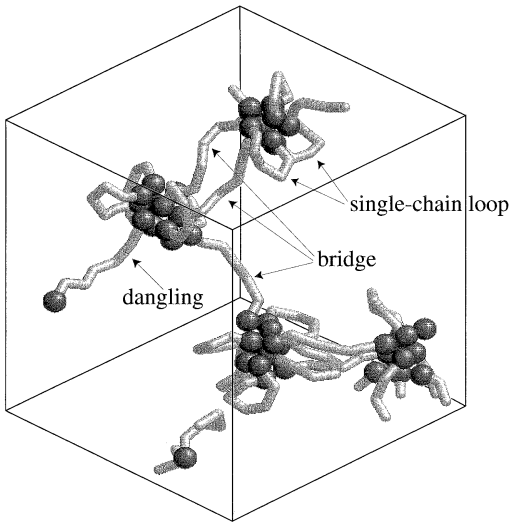

Fig. 4. Typical snapshot of network-forming telechelic AP solution. The bending constant is chosen as $k_\theta/k_BT = 5$.

can also be seen. By changing the temperature, or polymer concentration, we can see different types of aggregates. For instance, by increasing the polymer concentration at constant temperature, we can see that some loops open and change into bridge chains. A detailed description of such *loop/bridge transitions* is given below.

To find the gel point by MC, we plot the weight fraction of the largest cluster relative to the total weight of polymers as a function of the polymer concentration. Around a certain concentration, it sharply rises and asymptotically approaches a limiting value. We identify the gel point as the point where this curve passes an inflection point. Another theoretically equivalent, but practically different method is to find the concentration at which a cluster spans the simulation box, i.e., one end of the cluster is connected to the other end. In the following sections, we usually find the gel point by applying the second method, but we apply both whenever necessary.

3 Local and Global Structures of Networks

On passing the gel point, networks appear and coexist with finite clusters. The structure of a network can be studied from two different viewpoints: local viewpoint and global one. The local structure of a network focuses on the structure of each network junction, including its multiplicity, sequence length, degree of chain packing, etc., while the global structure treats topological connectivity of the network as a whole, paying special attention to the *cycle rank* (number of independent large loops), number of *elastically effective chains*, number of *dangling ends*, average *path number* of junctions, etc. Studies from such different viewpoints are complementary to each other, and both are necessary.

3.1 Structure of Cross-Link Junctions. When an associative group on a chain involves ζ sequential repeat units, we can write the standard free energy change as in Eq. 0.2. By taking the logarithm of the gelation concentration (2.11), we find an important relation

$$\ln \phi^* = \zeta \frac{\Delta h}{k_B T} + \ln \left[\frac{f' s' n}{f(f's' - 1)^{s/s'}} \right] - \zeta \frac{\Delta s}{k_B}. \qquad (3.1)$$

We can find multiplicity s and sequence length ζ by comparing this relation with the experimental sol/gel transition concentration. For the hydrophobes on associating polymers, the enthalpy Δh of a cross-link is found because ζ is known. For the micro-crystalline junction formed by homopolymers, each ζ sequence of repeat units along a chain surves as a functional group for cross-linking. In such a case, a polymer chain is regarded as carrying $f = n/\zeta$ functional groups. Since we have large n, and hence large f, we can neglect 1 compared to n or f, and are led to an equation

$$\ln c^* = \zeta \frac{\Delta h}{k_B T} - \frac{1}{s-1} \ln M + constant, \qquad (3.2)$$

for micro-crystalline gels, where weight concentration c^* has been substituted for the volume fraction. This equation enables us to find ζ and s independently. For the special case of pairwise association $s = 2$, this equation reduces to the conventional Eldridge–Ferry equation.[49]

Let us plot $\ln c^*$ against $10^3/T + \ln M$. Then the slope $-B$ of

the line at constant T gives $-1/(s-1)$, while the slope $-A$ of the line at constant M gives

$$\zeta = \frac{10^3 k_B}{|\Delta h|} A = \frac{10^3 R}{|(\Delta h)_{mol}|} A, \tag{3.3}$$

where $(\Delta h)_{mol}$ is the enthalpy of bonding per mole of the repeat units, and R the gas constant. We have applied this method to experimental data on the gel melting curves of several thermoreversible gels.[50] As an example of such analysis, we show in Fig. 5 the result for the gelation of poly(vinyl alcohol) (PVA) in water.[50] PVA is known to be a typical crystalline polymer, but it also gels in aqueous solution under large supercooling. There are several pieces of experimental evidence that the cross-links are formed by partial crystallization of the polymer segments in which syndiotactic sequence dominates, while subchains connecting the junctions consist mainly of atactic non-crystalline sequences on PVA chains. The micro-crystals at the junctions are supposed to be stabilized by hydrogen bonds between the hydroxy groups. We plot the gel melting temperature found from differential scanning calorimetry (DSC) and visco-elastic measurements for PVA with different molecular weights covering the range from 2×10^4 to 8×10^5 in various concentrations. The gel melting temperature T_m is estimated from the temperature at which the DSC heating curve shows an endotherm peak. The slope of the solid lines with constant molecular weight gives $-A = 13.43$ almost independently of their molecular weights. Hence we find $\zeta = 26.7$ kcal mol^{-1}/l$(\Delta h)_{mol}$l. If we use the heat of fusion $(\Delta h)_{mol} = 1.64$ kcal mol^{-1} in the bulk crystal, we find $\zeta = 16.3$. On the other hand, the slope of the dotted lines with constant temperature depends on the temperature. At the highest temperature $T = 91$ °C in the measurement, it is -0.38, while it gives a larger value -0.9 at $T = 71$ °C. The multiplicity is estimated to decrease from 3.6 for high-temperature melting to 2.1 for low-temperature melting, suggesting a very thin junction structure. From thermodynamic stability of the junctions it is only natural that a gel which melts at lower temperature has thinner junctions.

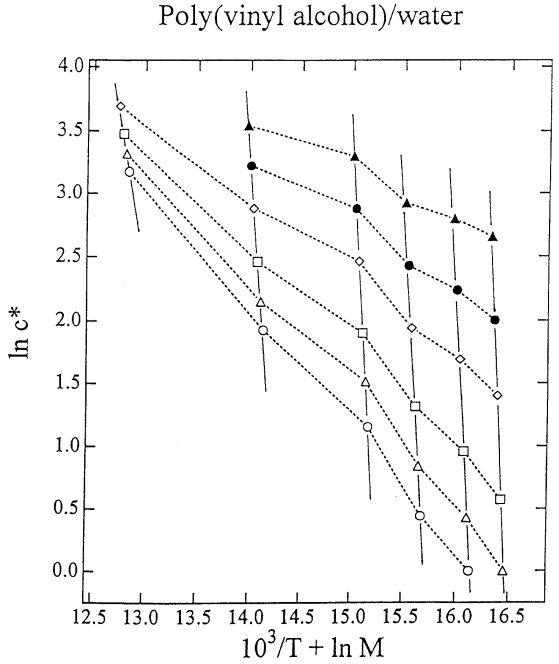

Fig. 5. Modified Eldridge-Ferry plot applied to the gel melting points of poly(vinyl alchohol)/water solution. Dotted lines connect the concentration at which gel melts at constant temperature, while thin straight lines show those at constant molecular weight. (▲) 91 °C; (●) 87 °C; (◇) 83 °C; (□) 78 °C; (△) 74 °C; (○) 71 °C.

3.2 Topological Connectivity of the Networks. To study visco-elastic properties of networks, we next find the number ν_{eff} of elastically effective chains.[36,51] The elastically effective chains are those chains that transmit stress when the network is deformed by external force. They are related to the topological structure of the network. Let us first specify the type of junctions from their connection paths to the network matrix.[52] A junction of multiplicity k that is connected to the network matrix through i paths is referred to as an (i,k)-junction. Let $\mu_{i,k}$ be the number of junctions in the network specified by the type (i,k) for $0 \le i \le 2k$ and for $k = 1,2,3,4,....$ The total number of junctions with multiplicity k is given by

$$\mu_k = \sum_{i=0}^{2k} \mu_{i,k}. \tag{3.4}$$

To find the number of elastically effective chains, we next employ the criterion of Scanlan[53] and Case.[54] It assumes that only subchains connected at both ends to junctions carrying at least *three paths* to the gel are elastically effective. We thus have $i,i' \ge 3$ for an effective chain. A junction with one path ($i = 1$) to the gel unites a group of subchains dangling from the network matrix whose conformations are not affected by an applied stress. A junction with two paths ($i = 2$) to the gel merely extends the length of an effective subchain. We may call a junction with $i \ge 3$ an *elastically effective junction*. An effective chain is defined as a chain connecting two effective junctions at both its ends. We thus find

$$\mu_{eff} = \sum_{k=2}^{\infty} \sum_{i=3}^{2k} \mu_{i,k} \tag{3.5}$$

for the number of elastically effective junctions, and

$$\nu_{eff} = \frac{1}{2} \sum_{k=2}^{\infty} \sum_{i=3}^{2k} i\mu_{i,k} \tag{3.6}$$

for the number of elastically effective chains.

A dangling end may consist either of a single subchain or of a group of subchains connected by several branch points. The structure of a dangling end can be described by the number of subchains and branch points it contains. By definition, the number of dangling ends is given by

$$\nu_{end} = \sum_{k=2}^{\infty} \sum_{i=2}^{2k} (2k - i)\mu_{i,k}. \tag{3.7}$$

The summation is taken over junctions with $i \ge 2$ because a junction with only one path to the gel is just a branch point on an already counted dangling end.

These topological relations hold for arbitrary networks. Their advantage lies in the fact that, by combinatorial counting,

we can actually find $\mu_{i,k}$ as a function of the degree α of association.[55] In our study, the degree α is found as a function of the temperature and concentration through the relation (2.5), so that all topological numbers described above can be calculated as functions of the temperature and concentration.[52] Figure 6 shows thus calculated numbers of elastically effective chains for telechelic AP ($f = 2$) with s varied from curve to curve as a function of α (Fig. 6(a)), and of the reduced concentration (Fig. 6(b)). Each curve rises in cubic power of the concentration deviation from the gel point and approaches unity at high limit of the concentration. It obeys the mean-field scaling law in the critical region

$$\nu_{\text{eff}}/\nu \simeq (\phi - \phi^*)^t \tag{3.8}$$

with $t = 3$. The cubic power comes of course from the mean-field treatment (tree statistics). According to percolation theory,[56] we should expect a smaller power $t = 1.7$. At the completion of the reaction $\alpha = 1$ (and hence $\lambda(T)\phi/n \to \infty$), the curves asymptotically reach unity. The number of effective chains is proportional to the polymer concentration in this region. These curves can be compared with the experimental data on the high frequency dynamic modulus measured by Annable et al.[2] Their experimental data for HEUR C16/35K (PEO end-capped with $C_{16}H_{33}$, molecular weight 35,000) are compared with our theoretical calculation[52] in Fig. 7. We have chosen as $c^* = 1.0\%$ for the weight concentration at gelation. With this gel concentration, the scaling power at the critical region gives $t = 1.6$, close to the percolation value. But since this power depends sensitively on the way we choose c^*, more detailed experimental examination in the critical region is eagerly required. In fitting the data, we have horizontally shifted the experimental data because of the temperature pre-factor $\lambda(T)$ and also because of the difference in the unit of the polymer concentration. Although fitting by a single theoretical curve is impossible due to the existence of polydispersity in the multiplicity, our theory produces correct behavior over a wide range of the concentration with multiplicity ranging from 6 to 8.

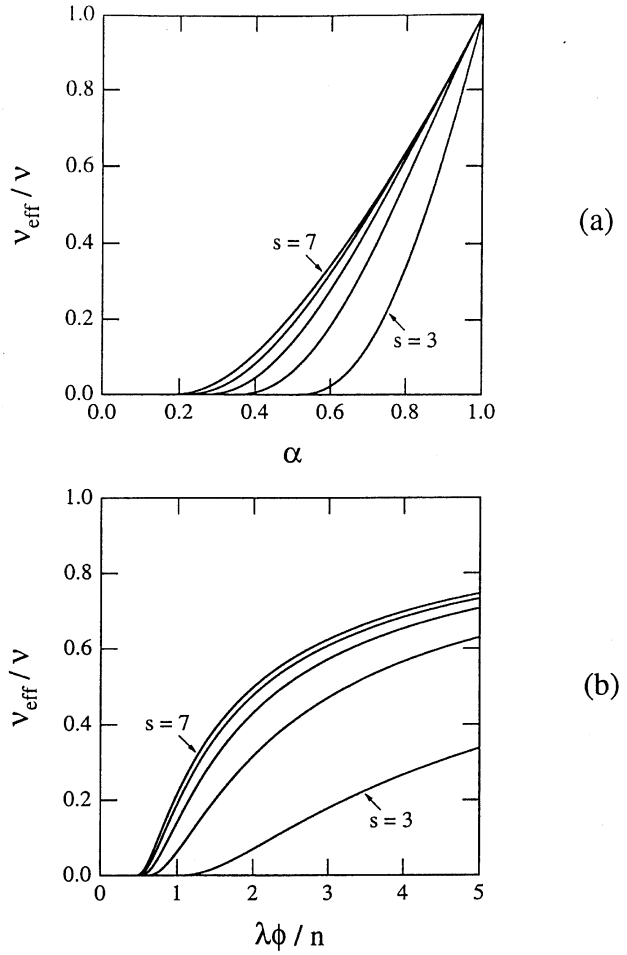

Fig. 6. The number of elastically effective chains (relative to the total number of chains) as a function of the extent of reaction (a), and of the reduced concentration (b).

4 Polymer–Surfactant Interaction

The interactions between polymers and surfactants have been a subject of great interest.[57,58] The problem was laid initially in studies of proteins associated with natural lipids, and later in the studies of their association with synthetic surfactants. More recently, interaction of water-soluble synthetic polymers such as poly(ethylene oxide) with ionic and non-ionic surfactants[59–62] have attracted the interest of researchers because of the scientific and technological implications. Adding surfactants to polymer solutions with formation of polymer/surfactant complex can substantially alter the physical properties of the starting polymers. The effects can be summarized into the following four categories: (i) Conformational transition of polymers such as coil-globule transition[63,64] and coil-rod transition,[65,66] (ii) Expansion and shift of the phase separation region on the polymer/solvent phase plane,[6] (iii) Forma-

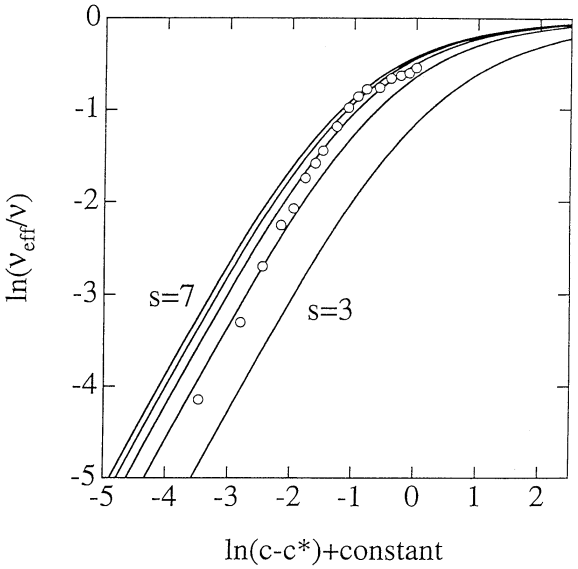

Fig. 7. Comparison of the high-frequency storage modulus of HEUR 16C/35K data measured by Annable et al. with theoretical calculation. Multiplicity is changed from curve to curve.

tion of composite microphases,[67] (iv) Shift of the sol/gel transition line[68–70] and modification of the rheological properties.[3,11,13] When polymers carry small fractions of hydrophobic groups, effects are dramatically enhanced, because the ability of surfactant binding is enhanced by the hydrophobic interaction between polymer hydrophobes and surfactant hydrophobes. A profound influence of added surfactants on the rheological properties has been reported. For example, the high-frequency plateau modulus of HEUR solution exhibits a large peak when sodium dodecyl sulfate (SDS) is added at low polymer concentrations. The peak in the modulus disappears at higher polymer concentrations.[3]

4.1 Theoretical Study of Polymer–Surfactant Interaction. To study the effect of added surfactants, we consider a model mixture of APs and low molecular-weight surfactant molecules in a solvent.[71] Each polymer is assumed to carry the number $f\,(\geq 2)$ of associative groups along its chain, and each surfactant molecule is modeled as a low molecular weight molecule carrying a single hydrophobe connected to the hydrophilic head. This is a special case of the model solution treated above.

In equilibrium, hydrophobes on the polymers and on the surfactants aggregate into mixed micelles that serve as cross-link junctions. The aggregation number differs from one micelle to another. If we use the (reduced) concentration $c_f \equiv \lambda(T)f\phi_f/n_f$ instead of ϕ_f for polymers and $c_1 \equiv \lambda(T)\phi_1/n_1$ for surfactants (n_i being the number of elementary statistical units on the molecule of species i), the relation (2.5) can be transformed into

$$c_f + c_1 = zu(z). \tag{4.1}$$

Solving this relation with respect to z for a given c_f and c_1, we find z, and hence the conversion α as a function of a given temperature and concentrations of both components.

The sol/gel transition condition for our polymer/surfactant system is then explicitly given by

$$(f-1)c_f zu'(z)/(c_f + c_1)u(z) = 1. \tag{4.2}$$

Combining this condition with the above relation and eliminating the parameter z, we find the sol/gel transition curve on the temperature-concentration plane.

When polymer concentration is low and the number of hydrophobes is not enough to form junctions, addition of surfactants combines the unassociated hydrophobes into forming stable junctions with aggregation number exceeding $s_{\min}$. In this situation, the surfactant works as a cross-linking agency. On the contrary, when the polymer concentration is large and many junctions are already formed, some of the polymer hydrophobes in the junctions are replaced by surfactant hydrophobes as soon as their multiplicity reaches $s_{\max}$, leading to the dissociation of network junctions.

To demonstrate these opposite effects, we calculate the concentration of polymers at the sol/gel transition point as a function of the concentration of the added surfactant.[71] Figure 8 shows the result for the telechelic ($f = 2$) polymers. Both polymer and surfactant concentrations are expressed in terms of the reduced concentration, the number of hydrophobes (per lattice cell) times association constant. To see the effect of the minimum multiplicity, $s_{\min}$ is varied from curve to curve, while the maximum multiplicity is fixed at $s_{\max} = 8$. It is clear that the sol/gel concentration c^*_f monotonically increases with the surfactant concentration for $s_{\min} = 2$ (no lower bound), i.e., gelation is simply blocked by the surfactant. But if there is a forbidden region between $k = 1$ (unassociated) and $k = s_{\min}$, a minimum in c^*_f starts to appear. At this surfactant concentration gelation is most promoted as can be seen for $s_{\min} \geq 3$. The surfactant concentration at which c^*_f becomes minimum is referred to as the *surfactant-mediated gelation* (SMG) point. It increases as the minimum multiplicity becomes larger.

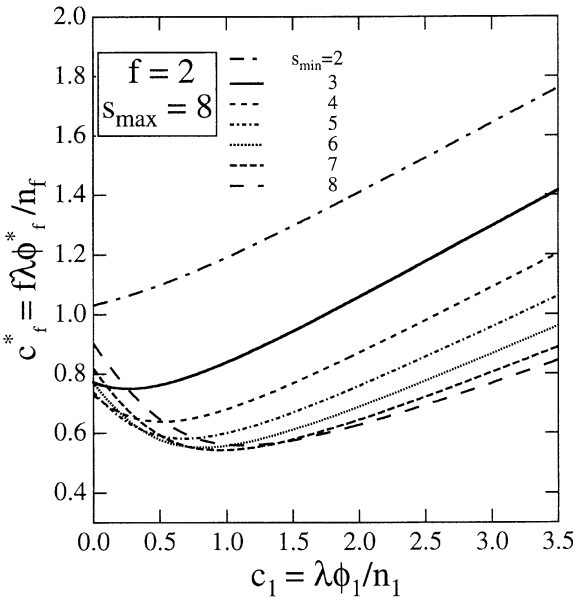

Fig. 8. Polymer concentration at sol/gel transition as a function of the concentration of added surfactant. Minimum multiplicity $s_{\min}$ is varied from curve to curve under a fixed maximum multiplicity $s_{\max}$.

4.2 CMC of the Surfactant Molecules. Surfactant molecules form micelles above a certain concentration. The concentration at which micelles start to appear is referred to as the *critical micelle concentration* (CMC). To see how CMC is affected by the presence of associating polymers, let us focus on the surfactant molecules that are not associated to any polymers.

The clusters consisting purely of surfactant molecules are indicated by $l_f = 0$, so that we have $\mathbf{l} = \{l_1, 0\}$. There is a single junction of the multiplicity $k = l_1$ in such a pure surfactant cluster. We then have $j_k = 1$ for $k = l_1$ and other $j_k = 0$. The distribution function becomes

$$\lambda\nu(\mathbf{j};\mathbf{l}) = \gamma_{l_1}(x_1)^{l_1}/l_1. \tag{4.3}$$

The total volume fraction of the pure surfactant micelles is given by

$$\lambda\phi_1^{\mathrm{iso}}/n_1 \equiv \lambda \sum_{l_1 \geq 1} l_1 \nu(\mathbf{j};\mathbf{l}) = x_1 u(x_1). \tag{4.4}$$

Since $x_1 = c_1(1-\alpha) = c_1/u(z)$ by definition, we find

$$\lambda\phi_1^{\mathrm{iso}}/n_1 = c_1 u(x_1)/u(z). \tag{4.5}$$

From this result, we find that the surfactant molecules adsorbed into junctions made up of polymer hydrophobes is given by

$$\phi_1^{\mathrm{ads}} = [1 - u(x_1)/u(z)]\phi_1. \tag{4.6}$$

The adsorption probability θ (the probability for a surfactant molecule to be attached to a junction in a cluster) is therefore given by

$$\theta = 1 - u(x_1)/u(z). \tag{4.7}$$

In our mixture, we define the critical micelle concentration by the surfactant concentration at which micelles consisting only of surfactant molecules start to appear. In what follows we refer to this concentration as the *critical pure micelle concentration* (CPMC). One conventional criterion for CMC is to find the concentration at which the osmotic pressure changes its slope most rapidly.[72] This criterion is almost equivalent to the condition that the weight density of the surfactant molecules expressed as a function of that of the isolated (unassociated) molecules ceases to have its inverse function.[72] In our present particular model, this happens when

$$\mathrm{d}(zu(z))/\mathrm{d}z = u(z) + zu'(z) = 0 \tag{4.8}$$

holds. This equation is an algebraic equation for z and has its roots on the complex z-plane. These roots are branch points of the inverse function. When the concentration x_1 of the unassociated surfactant passes near the root that lies closest to the real z-axis, the osmotic pressure due to surfactant molecules changes its slope most rapidly.

To study the relative position of CPMC and SMG concentration, we consider a special multiplicity model in which junction multiplicity is fixed at a single value s. The function $u(z)$ in this fixed multiplicity model takes the form $u(z) = 1+z^{s-1}$ by definition

The top figure in Fig. 9 shows sol/gel transition line (solid line) and CPMC line (broken line) on the triangular plane of polymer/surfactant/water system. SMG and the point where CPMC line and the gel line cross are indicated by the black circle and the open one. Their relative position may change if we allow differences in the binding free energies for a polymer hydrophobe and for a surfactant hydrophobe into the micelles.

4.3 Enhancement of Elastic Modulus. We next study the effect of added surfactants on the dynamic mechanical moduli of AP solution. In the experiment of HEUR/SDS system,[3] addition of surfactant results in several effects. The moduli can no longer be described by the simple Maxwell element with a single relaxation time, but a shoulder appears on the loss modulus at high frequencies. The high frequency plateau in the storage modulus reveals non-monotonic dependence on the SDS concentration. At low polymer concentration, it initially rises to a peak and then decreases monotonically, falling eventually to zero at higher SDS concentration. With increase in the polymer

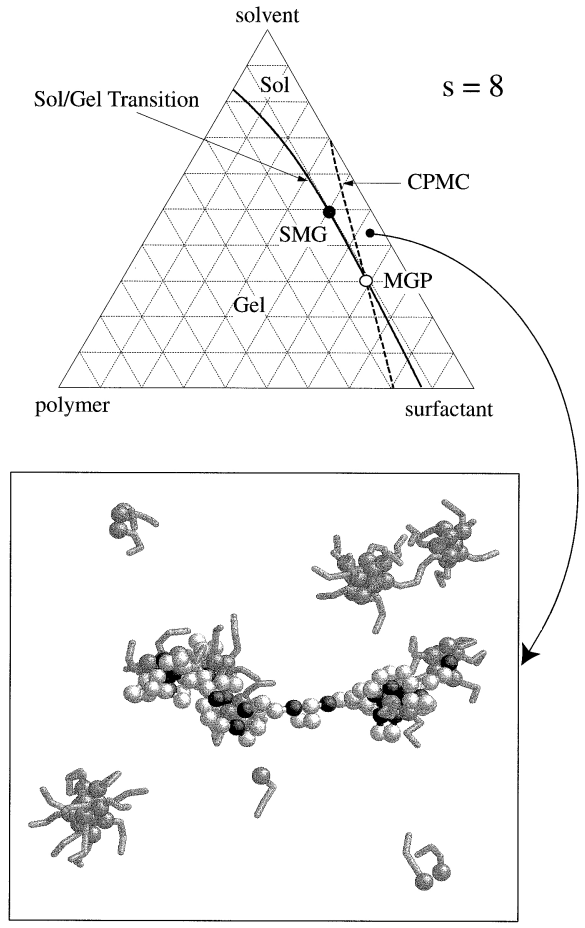

Fig. 9. (top) The sol/gel transition line and the CPMC line drawn on the ternary phase plane of polymer/surfactant/solvent system. The minimum gelation point is indicated by a black circle. The white circle shows a special point at which gelation and micellization simultaneously take place. (bottom) Snapshot of MC in which a periodic AP undergoes conformational transition induced by adsorption of surfactant molecules.

concentration, the height of the peak in the storage modulus decreases and its position shifts to lower SDS concentration. Above a certain polymer concentration, the peak disappears.

The plateau value of $G'(\omega)$ is expected to be proportional to $\nu_{\mathrm{eff}}(c_1)k_{\mathrm{B}}T$ because the network topology does not alter within the measurement timescale ω^{-1}, which is shorter than the average lifetime τ_{x} of a junction. Therefore, we can study the elastic moduli by counting the number of elastically effective chains as a function of the concentration of surfactant. Figure 10 shows the number $\nu_{\mathrm{eff}}(c_1)$ plotted against the surfactant concentration c_1 (divided by the polymer concentration c) for $f = 2$. The number is normalized by the value $\nu_{\mathrm{eff}}(0)$ under the absence of the surfactant. This ratio gives the relative amplitude $G'(c_1)/G'(0)$ of the high frequency plateau value in the storage modulus. The multiplicity of a junction is varied from 3 to 8. The polymer concentration $c_{f=2}$ is changed from curve to

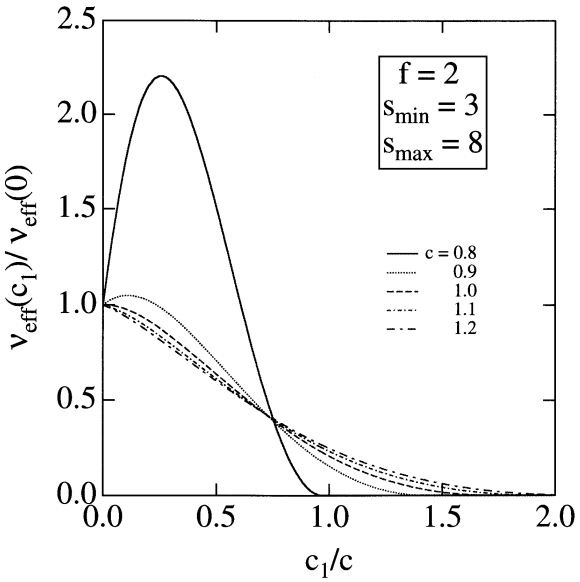

Fig. 10. High frequency plateau modulus as calculated from the number of elastically effective chains plotted against the concentration of added surfactant. Curves for low polymer concentrations show a peak at a certain surfactant concentration.

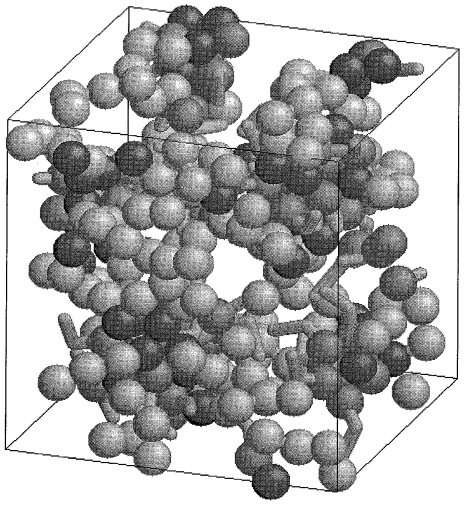

Fig. 11. MC snapshot of telechelic AP solution mixed with surfactant molecules. New junctions of mixed micelles are created by the help of surfactant molecules, leading to more chances for polymers to form networks.

curve. As expected, the curves of the number of elastically effective chains for low polymer concentrations first rise to a peak and then monotonically decrease to zero where the gel network is broken into sol by the surfactant. For higher polymer concentrations, however, the curves do not show any peak, because junctions are well developed without surfactant molecules for such polymer concentrations and the added surfactant merely destroys junctions.

These calculations reproduce, at least qualitatively, the experimental data on such as HEUR/SDS reported by Annable et al.[3] However, in our theory, all curves cross each other at a certain surfactant concentration, whereas the experimental data reveal the same tendency only for relatively high polymer concentrations. The maximum in the modulus is caused by the existence of a forbidden region in the multiplicity of the network junctions.

4.4 Polymer–Surfactant Interaction as Studied by MC Simulation. To see the two opposite effects of surfactant mentioned above, we have performed MC simulation on AP mixed with surfactant. A surfactant molecule is modelled as a one-end functional low molecular weight molecule. In the bottom figure of Fig. 9, a periodic AP with period 4 carrying a total of 81 beads is shown to undergo conformational transition from compact micelles to elongated trains of mixed micelles by adsorbing surfactant molecules consisting of 3 beads. The concentration of surfactant lies above its CPMC as shown in the ternary diagram because three pure micelles of surfactant are formed in the simulation box.

Figure 11 shows a typical snapshot of MC simulation on telechelic polymers of 7 beads mixed with surfactant molecules of 3 beads at concentrations $\phi_2 = 0.1$ and $\phi_1 = 0.08$. Surfactant molecules create new junctions by forming mixed micelles. In other words, they serve as cross-linkers, or *gluons* working among polymer hydrophobes. Gelation is promoted, so that the polymer concentration at the gel point is lowered.

5 Effect of Loop Formation

Let us turn back to AP solutions. We have so far excluded the effect of loop formation in the clusters. We now try to take such loops into consideration. Loops are roughly classified into two categories; small loops and large loops. Small loops are those formed within a single chain. The association among functional groups in a single chain forming flower-like micelles with small loops (*petals*) as shown in Fig. 2 is called *intramolecular association*. Large loops involve many (at least more than two) chains. The number of large loops in a cluster is called its *cycle rank* in the literature,[51] and plays an important role in rubber elasticity of polymer networks. We consider here the former ones. In a solution, intramolecular and intermolecular association compete with each other. Frequencies of their occurrence change with temperature and concentration. Assuming perfect equilibrium in association, we can study association by splitting the process into two stages. In the first stage, we consider how intramolecular association takes place. A chain generally carries several flowers, whose cores serve as composite associative groups if they are not saturated. It can also be regarded as an excited state in its conformational space. In the second stage, we connect these excited chains with each other to form clusters and networks. We can thus study how the relative population of bridge chains and petal chains changes with concentration.

5.1 Six Types of Association in Telechelic Associating Polymers. To clarify the problem, let us consider telechelic polymers. The excited state of telechelic polymers is unique, namely, a single loop. The probability to form such a loop is decided by the thermodynamic equilibrium condition, and is

given by

$$\zeta = B\lambda(T)/n^{3/2}, \tag{5.1}$$

where $\lambda(T)$ is the association constant, n the total number of the statistical units on a chain, and B some numerical constant.[73] Strictly, the power 3/2 in Eq. 5.1 should be replaced by $d\nu+\gamma-1$ for polymers in a good solvent, where $d = 3$ is the space dimension, $\nu = 3/5$ the Flory's exponent, and $\gamma = 7/6$ is the critical exponent describing the total number of self-avoiding random walks.[74] However, we neglect the excluded-volume effect throughout this paper since our solution theory and gelation theory are both based on the mean-field treatment. We introduce the parameter ζ as a new parameter independent of the association constant λ.

The loop parameter (5.1) can also be written as

$$\zeta = \exp(-\beta\Delta A), \tag{5.2}$$

where $\Delta A \equiv A_1 - A_2$ is the difference in the conformational free energy between the reference conformation (open chain with two unassociated groups, indicated by the subscript 2) and the excited conformation (a loop with a single composite associative group, indicated by the subscript 1). Thermoreversible gelation strongly coupled to such an internal conformation change can be treated more generally by including polymers carrying arbitrary numbers of associative groups. Details of the theory are reported in our recent paper.[75]

A loop is regarded as a pseudomolecule carrying a single effective associative group formed by the doublet of the original associative groups. We then have the model solution in which bifunctional telechelic polymers are mixed with monofunctional loops. Thus our problem can be mathematically mapped onto the mixture of the associating polymers and surfactant molecules that was already studied in the preceding section. The only difference lies in that the population of loops (corresponding to surfactants) is automatically controlled by the thermodynamic equilibrium condition. We can thus study the effect of small loops on the gelation of AP within the scheme of classical tree statistics.

For our present chain/loop mixture, the total number density of the associative groups is given by $\Psi = (\phi_1 + 2\phi_2)/n$, where ϕ_f (f = 1,2) is the volume fraction of the loops (f = 1) and of the chains (f = 2). The total volume fraction ϕ of the polymers in the solution is given by $\phi = \phi_1+\phi_2$. The number density of each molecule is given by $\nu_f = \phi_f/n$. In the surfactant problem, these densities are fixed at the preparatory stage of the experiment, but here their relative population is decided by the equilibrium loop parameter ζ as

$$\nu_1^\circ/\nu_2^\circ = \zeta, \tag{5.3}$$

where the superscript $^\circ$ indicates that ν°_f is the number density of molecules in the conformation with f that remain isolated in the solution. By definition, we have $\nu^\circ_f = \nu_f(1-\alpha)^f = \nu_f/u(z)^f$. Hence, the relation

$$\phi_1/\phi_2 = \zeta/u(z) \tag{5.4}$$

holds. On substitution into (2.5), we find

$$\left(\frac{\lambda}{n}\phi\right)\frac{\zeta+2u(z)}{\zeta+u(z)} = zu(z), \tag{5.5}$$

so that the number-average functionality $<f>$ of the loop/chain mixture turns out to be given by

$$<f> = [\zeta+2u(z)]/[\zeta+u(z)], \tag{5.6}$$

which depends on the polymer concentration.

At this stage, it should be noted that in our treatment of (2.5) an original associative group on a chain and a composite associative group on a loop are assumed to have the same association constant $\lambda(T)$. Strictly, the latter has a different association constant $\mu(T)$ because the free energy produced on binding the composite group into a miceller junction is different from that for the original group. We assume, however, they are the same to avoid complexity in this paper.

To see how closed association changes into open association, we first summarize all possible types of the chains in the solution. There are 6 categories altogether. They are shown in Fig. 12, i.e., isolated open chain, isolated loop, cluster consisting only of loops (called "*flower micelles*"), bridge chain, dangling chain, dangling loop in a cluster. In what follows we pay special attention to the pure flowers, and the concentration of their appearance (referred to as "*critical flower micelle concentration*" CFMC). Specifically we ask whether CFMC of flowers lies below or above the gel concentration. The answer depends on the parameter ζ.

First, the volume fraction of unassociated open chains is given by $\phi_2(1-\alpha)^2$, so that their fraction among the total chains is given by $C_0 = \phi_2(1-\alpha)^2/\phi$. It should be remarked that the conversion α in this equation is the degree of association when the

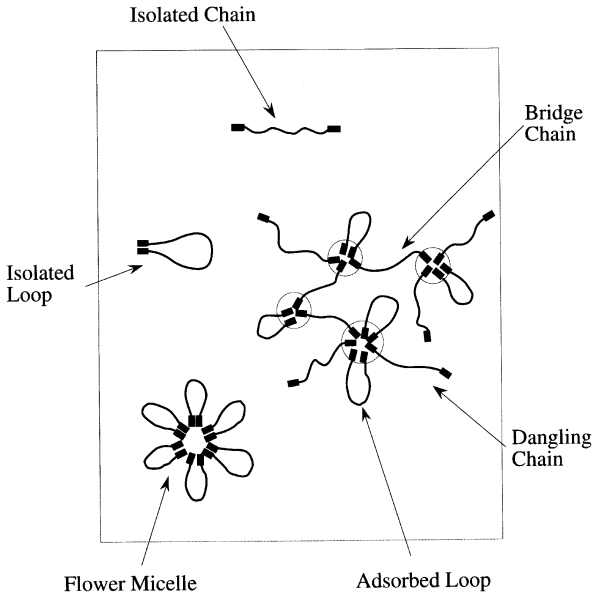

Fig. 12. Six chain categories in telechelic associating polymer solution. They are: isolated chain, isolated loop, flower loop, bridge chain, dangling chain, adsorbed loop.

composite group (doublet) carried by a loop is regarded as a single effective associative group. The true conversion α_0 regarding the original groups is different from this, and is given at the end of this section.

The fraction of the loops that remain isolated in the solution is given by $L_0 = \phi_1(1 - \alpha)/\phi$. Similarly, the fraction of dangling chains and of bridge chains in the clusters are given by $C_d = 2\phi_2\alpha(1 - \alpha)/\phi$ and $C_b = \phi_2\alpha^2/\phi$.

Finally, let us consider loops again. A loop is either isolated, or attached to a cluster junction, or belongs to a flower micelle. In the previous section, we studied the adsorption probability θ of surfactant molecules into polymer clusters. It was found to be given by Eq. 4.7. In the present context, c_1 corresponds to the volume fraction (times association constant) of the unassociated loops. The fraction of the loops dangling from the cluster junctions is then given by $L_{ad} = \phi_1\theta/\phi$. The fraction of the loops that belong to the flower micelles is then given by subtraction as $L_f = \phi_1(\alpha - \theta)/\phi$.

The conversion α used so far is the superficial degree of association calculated under the assumption that the composite group on a loop is regarded as one associative group. The real conversion α_0 is, however, defined by the number of associated functional groups divided by the total number of groups. Therefore, it is given by $\alpha_0 = 2(\phi_1 + \phi_2\alpha)/2(\phi_1 + \phi_2) = [\alpha + \zeta(1 - \alpha)]/[1 + \zeta(1 - \alpha)]$. As a function of the loop parameter ζ, it starts from α and monotonically increases to unity. Figure 13 shows the relative population of each chain category as a function of the total polymer concentration. The multiplicity of junctions is allowed in the range between $s_{min} = 5$ and $s_{max} = 8$ for a fixed loop parameter $\zeta = 5$. Curves are normalized to give unity when summed up. Isolated loops and isolated chains start with the ratio 5 to 1, but both of them decrease with the polymer concentration, because they are adsorbed into mixed clusters. Dangling chains, adsorbed loops, and bridge chains increase with the concentration, but bridge chains eventually dominate at high concentrations. Flower loops appear in a certain range of the concentration. Their curve exhibits a single maximum around $c = 1.5$. Since the gelation concentration for this solution is given by $c^* = 2.2$, flowers appear before the solution gels.

5.2 The Flower/Bridge Transition. Let us next consider the volume fraction $\phi_{fl} = L_f\phi$ of the flower micelles. Figure 14 shows a snapshot of a flower micelle obtained in MC. The non-associative beads are replaced by bonds in the bottom figure. Since the parameters z and x_1 are given as a function of the total polymer concentration, we find ϕ_{fl} as a function of the concentration. By differentiation, the concentration at which the volume fraction of flowers become maximum satisfies the condition $dx_1/dc = 0$. This is equivalent to the condition for the gel point. We thus find within our theoretical scheme that the concentration of flower micelles reaches a maximum value at the gel point.

The concentration at which ϕ_{fl} rises from zero is CFMC. Since it increases very slowly with total polymer concentration, the conventional method to identify CMC from the point where the population curve of the micelles sharply bends is not directly applicable. As a rough estimate, we here employ a criterion that the concentration where the absolute value of ϕ_{fl} reaches a certain threshold value is CFMC. The actual value of the CFMC obtained in this simple method depends sensitively upon the chosen threshold value. We have fixed this value at $\phi_{fl} = 0.001$, although it is somewhat arbitrary. The result is shown in Fig. 15 together with the gelation line. For small values of the loop parameter, the solution gels without flower micelles, but above a certain value of the loop parameter, there is a large

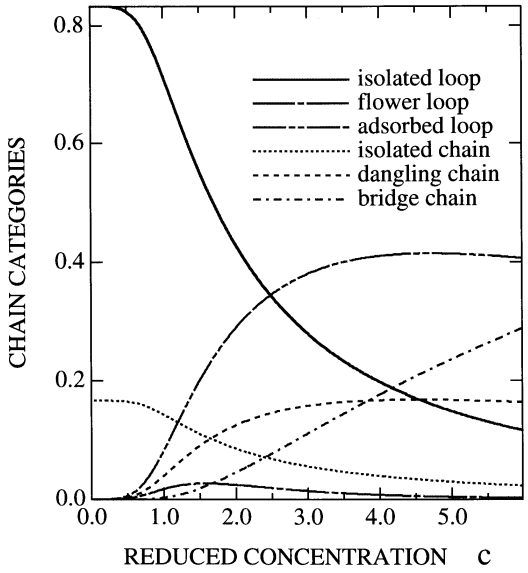

Fig. 13. Relative population of each chain category plotted against total polymer concentration. The loop parameter is fixed at $\zeta = 5$. The allowed multiplicity is limited by $s_{min} = 5$ and $s_{max} = 8$. The gelation concentration for this solution is given by $c^* = 2.2$.

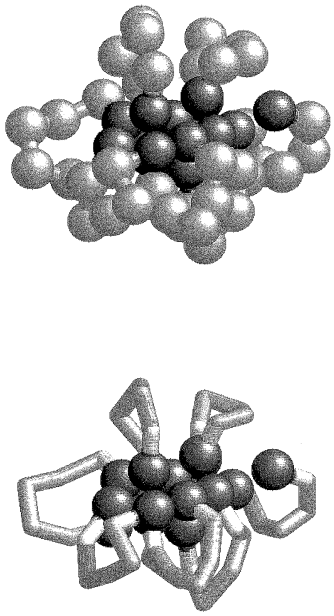

Fig. 14. A flower micelle obtained in MC shown with and without non-associative beads.

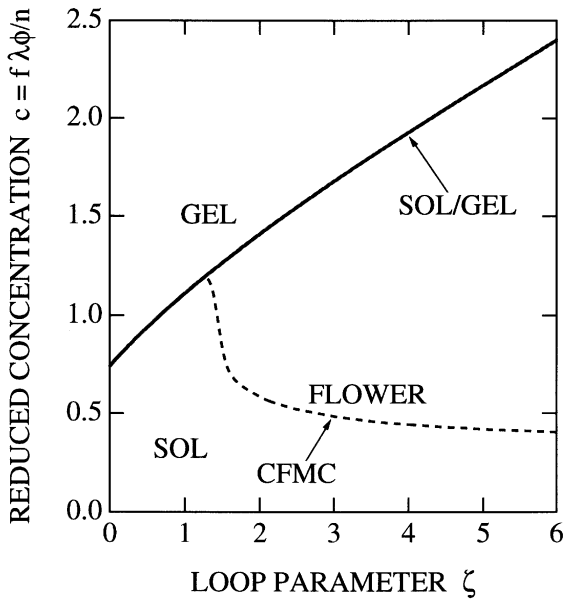

Fig. 15. Phase diagram showing the domains of flower micelles and gels. When the loop parameter becomes larger than a critical value, flower micelles are formed before gelation. There is a region on the phase plane in which flower micelles are dominant.

region of flowers. Hence many flowers are formed before the solution gels.

In MC simulation, the appearance of flower micelles depends, of course, upon the bending constant k_θ. Flexible polymers with $k_\theta = 0$ easily form flowers, but polymers with finite k_θ can also form flowers once cores of aggregates reach an appreciable size even if their loop parameter is small (see Fig. 4). Such an acceleration effect in loop formation is not seen in the theory because the free energy for binding an associative group is assumed to remain constant irrespective of the aggregation size. In a simulation, loops eventually change into bridge chains with increase in the polymer concentration before the gel point is reached.

6 Conclusions and Discussion

We have presented an outline of our recent theoretical and computational studies on thermoreversible gelation in polymer solutions with network junctions of variable multiplicity. Thermodynamic nature of the sol/gel transition, interference with phase separation, structure of the network junctions, path connectivity in the network have been studied on the basis of the multiple tree statistics combined with classical lattice-theoretical polymer solutions. The effect of loop formation within a cluster has also been elucidated though under very limited conditions. Our studies have mainly focused on the gelation of water-soluble associating polymers driven by hydrophobic aggregation, but find application to experimental data on other types of gels such as those driven by hydrogen bonding, micro-crystallization etc. Further modifications and applications of our theory and simulation would involve the following important gelling solutions:

Hydration and High-Temperature Gelation. Natural polymers often gel on heating. A typical example which has long been under intensive scrutiny is methyl cellulose with a nearly full degree of molar substitution by methoxy groups.[16,27] In an aqueous solution at low temperatures, polymer chains are covered with water molecules attached by hydrogen bonds (*hydration*) so that direct association between polymer segments is prohibited. As the temperature is raised, chains gradually lose attached waters, and polymer–polymer association, which is initiated by hydrophobic interaction, being stabilized by direct hydrogen bonds, begins to take place. As dehydration proceeds, the number of direct interchain associations increases and eventually reaches a critical value for the formation of an infinite network of polymers. The gel liquefies to the original constituency on cooling.[16] Because the hydrophobic segments on polymer chains are partly exposed to water in the gel regime, the solution tends to separate into two macroscopic phases. Thus gelation and phase separation compete as the temperature goes up. We have theoretically derived phase diagrams with high-temperature gels[76] by taking hydration of water molecules into account. Our theory predicted a diverse variety of phase diagrams depending on the relative strength of the polymer-polymer association and polymer–solvent association.

Gelation Strongly Coupled to Polymer Conformational Transition. Natural polymers also undergo conformational transition preceding gelation, thereby activation of the particular functional groups on a polymer chain accompanied by proper three dimensional conformation change is a necessary prerequisite for the interchain cross-linking. For instance, water-soluble natural polymers such as agarose and κ-carrageenan first change their conformation from the random coil state to a partially helical state, and then the helical parts aggregate to form network junctions.[23,24,27,28,77] Recently, a similar two-step mechansim of gelation through coil-to-helix transition was confirmed for synthetic polymers with stereo-regularity.[78,79]

Other important examples are globular proteins. Proteins such as ovalbumin, or human serum albumin, are believed to form gels after some of the intramolecular bonds in a native state are broken during denaturation, with their functional groups being exposed to the outer space, followed by the intermolecular recombination of the groups.[24,80,81] A certain degree of unfolding to expose functional groups is a necessary condition for the gelation in these examples.

We have studied[75] the effects of polymer conformational change on the thermoreversible gelation of natural and synthetic polymers by introducing conformational free energy in addition to our starting model free energy (2.1). Gelation is classified into two major types: high-temperature gelation and low-temperature gelation. Transition from intra- to intermolecular bonding due to denaturation of some proteins leads to the former type, while coil to helix transition and coil to rod transition lead to the latter. Typical phase diagrams in which sol/gel transition and phase separation coexist are derived to study how they depend upon the nature of the polymer conformational change. We found that selection of sequences for helix for-

mation from a linear chain is strongly correlated with the junction multiplicity, but many questions remain open.

Gelation of Stiff Chains. As discussed in the text, chain stiffness significantly affects the structure of aggregates; it prevents loop formation, induces orientational ordering through excluded-volume interaction, and leads to formation of bundles made up of parallel chains. Gelation competing with liquid-crystalline ordering is another important problem yet to be studied. Network formation by rod-like molecules with associative groups at both ends, for instance, is one of the simplest systems that our theory and simulation can cover.

It is hoped to pursue these topics in later publications. We intend also to investigate dynamic and rheological properties of transient networks formed by physical cross-linking, as well as to attempt a more detailed comparison of our theoretical and computational studies with experimental data.

This work was partly supported by Grant-in-Aids for Scientific Research (C)(09650987) and (B)(12450387) from the Ministry of Education. F.T. would like to thank Professor W. H. Stockmayer, Professor S. F. Edwards, and Dr. M. Ishida for collaborations during the last decade. The authors thank Mr. T. Furuya for offering them a MC snapshot of polymers interacting with surfactant molecules.

References

1 M. A. Winnik, *Curr. Opin. Colloid Interface Sci.*, **2**, 424 (1997).
2 T. Annable, R. Buscall, R. Ettelaie, and D. Whittlestone, *J. Rheol.*, **37**, 695 (1993).
3 T. Annable, R. Buscall, R. Ettelaie, P. Shepherd, and D. Whittlestone, *Langmuir*, **10**, 1060 (1994).
4 B. Rao, Y. Uemura, L. Dyke, and P. M. Macdonald, *Macromolecules*, **28**, 531 (1995).
5 E. Alami, M. Almgren, W. Brown, and J. Francois, *Macromolecules*, **29**, 2229 (1996).
6 E. Alami, M. Almgren, and W. Brown, *Macromolecules*, **29**, 5026 (1996).
7 B. Xu, A. Yekta, and M. A. Winnik, *Langmuir*, **13**, 6903 (1997).
8 Z. Zhou, Y. Y-W., C. Booth, and B. Chu, *Macromolecules*, **29**, 8357 (1996).
9 E. J. Amis, N. Hu, T. A. P. Seery, T. E. Hogen-Esch, T. E., M. Yassini, and F. Hwang, in "Hydrophobic Polymers: Performance with Environmental Acceptance," ed by E. Glass, Am. Chem. Soc. (1996), p. 279.
10 F. S. Hwang and T. E. Hogen-Esch, *Macromolecules*, **28**, 3328 (1995).
11 X. Xie and T. E. Hogen-Esch, *Macromolecules*, **29**, 1734 (1996).
12 H. Zhang, J. Pan, and T. E. Hogen-Esch, *Macromolecules*, **31**, 2815 (1998).
13 S. Nilsson, *Macromolecules*, **28**, 7837 (1995).
14 B. Nyström, K. Thuresson, and B. Lindman, *Langmuir*, **11**, 1994 (1995).
15 B. Nyström, H. Walderhaug, F.K. Hansen, and B. Lindman, *Langmuir*, **11**, 750 (1995).
16 N. Sarkar, *J. Appl. Polym. Sci.*, **24**, 1073 (1979).
17 K. Kobayashi, C. Huang, and T. P. Lodge, *Macromolecules*, **32**, 7070 (1999).
18 Y. Morishima, *Trends in Polym. Sci.*, **2**, 31 (1994).
19 Y. Morishima, S. Nomura, T. Ikeda, M. Seki, and M. Kamachi, *Macromolecules*, **28**, 2874 (1995).
20 F. Petit, I. Iliopoulos, R. Audebert, and S. Szonyi, *Langmuir*, **13**, 4229 (1997).
21 G. Bokias, D. Hourdet, I. Iliopoulos, G. Staikos, and R. Audebert, *Macromolecules*, **30**, 8293 (1997).
22 G. Bokias, D. Hourdet, and I. Iliopoulos, *Macromolecules*, **33**, 2929 (2000).
23 W. Burchard, *British Polym. J.*, **17**, 154 (1985).
24 A. H. Clark and S. B. Ross-Murphy, *Ad. Polym. Sci.*, **83**, 57 (1987).
25 P. S. Russo, "Reversible Polymeric Gels and Related Systems," American Chemical Society, Washington DC (1987), Vol. 350.
26 O. Kramer, "Biological and Synthetic Polymer Networks, Elsevier Applied Science," London and New York (1988).
27 J. M. Guenet, "Thermoreversible Gelation of Polymers and Biopolymers," Academic Press, Harcourt Brace Jovanovich Publishers (1992).
28 K. te Nijenhuis, *Ad. Polym. Sci.*, **130**, 1 (1997).
29 K. C. Tam, R. D. Jenkins, M. A. Winnik, and D. R. Bassett, *Macromolecules*, **31**, 4149 (1998).
30 F. Tanaka and S. F. Edwards, *Macromolecules*, **25**, 1516 (1992).
31 F. Tanaka and S. F. Edwards, *J. Non-Newtonian Fluid Mech.*, **43**, 247, 272, 289 (1992).
32 K. Fukui and T. Yamabe, *Bull. Chem. Soc. Jpn*, **40**, 2052 (1967).
33 F. Tanaka and W. H. Stockmayer, *Macromolecules*, **27**, 3943 (1994).
34 P. J. Flory, *J. Chem. Phys.*, **12**, 425 (1944).
35 M. L. Huggins, *J. Chem. Phys.*, **46**, 151 (1942).
36 P. J. Flory, "Principles of Polymer Chemistry," Cornell University Press (1953).
37 F. Tanaka and T. Koga, *Comp. Theor. Polym. Sci.*, **10**, 259 (2000).
38 K. Binder, A. Milchev, and J. Baschnagel, *Ann. Rev. Mater. Sci.*, **26**, 107 (1996).
39 N. Metropolis, A. W. Rosenbluth, M. N. Rosenbluth, and A. H. Teller, *J. Chem. Phys.*, **21**, 1087 (1953).
40 R. J. Baxter, *J. Chem. Phys.*, **49**, 2770 (1968).
41 J. Xu and G. Stell, *J. Chem. Phys.*, **89**, 1101 (1988).
42 W. G. T. Kranendonk and D. Frenkel, *Molecular Physics*, **64**, 403 (1988).
43 F. Tanaka, *Macromolecules*, **23**, 3784, 3790 (1990).
44 P. J. Flory, *J. Am. Chem. Soc.*, **63**, 3091, 3096 (1941).
45 W. H. Stockmayer, *J. Chem. Phys.*, **11**, 45 (1943); *J. Chem. Phys.*, **12**, 125 (1944).
46 C. M. Knobler and R. L. Scott, in "Phase Transitions and Critical Phenomena," Academic Press, New York (1984), Vol. 9.
47 F. Tanaka, *Phys. Rev. Lett.*, **68**, 3188 (1992).
48 A. Kikuchi and T. Nose, *Macromolecules*, **29**, 6770 (1996).
49 J. E. Eldridge and J. D. Ferry, *J. Phys. Chem.*, **58**, 992 (1954).
50 F. Tanaka and K. Nishinari, *Macromolecules*, **29**, 3625 (1996).
51 P. J. Flory, *Proc. R. Soc. London, Ser. A*, **351**, 351 (1976).
52 F. Tanaka and M. Ishida, *Macromolecules*, **29**, 7571 (1996).
53 J. Scanlan, *J. Polym. Sci.*, **43**, 501 (1960).

54 L. C. Case, *J. Polym. Sci.*, **45**, 397 (1960).
55 D. S. Pearson and W. W. Graessley, *Macromolecules*, **11**, 528 (1978).
56 D. Stauffer, "Introduction to Percolation Theory," Taylor & Francis, London (1985), Chap. 2.
57 "Microdomains in Polymer Solutions," ed by P. Dubin, Plenum Press, New York (1985).
58 "Interactions of Surfactants with Polymers and Proteins," ed by E. D. Goddard and K. P. Ananthapadmanabhan, CRC Press, Boca Raton, FL (1993).
59 B. J. Cabane, *J. Phys. Chem.*, **81**, 1639 (1977).
60 W. Brown, J. Fundin, and M. da Graça ca Miguel, *Macromolecules*, **25**, 7192 (1992).
61 E. Feitosa, W. Brown, and P. Hansson, *Macromolecules*, **29**, 2169 (1996).
62 E. Feitosa, W. Brown, M. Vasilescu, and M. Swason-Vethamuthu, *Macromolecules*, **29**, 6837 (1996).
63 J. Rička, M. Meewes, R. Nyffenegger, and T. Binkert, *Phys. Rev. Lett.*, **65**, 657 (1990).
64 M. Meewes, J. Ricka, M. de Silva, R. Nyffenegger, and T. Binkert, *Macromolecules*, **24**, 5811 (1991).
65 G. H. Fredrickson, *Macromolecules*, **26**, 2825 (1993).
66 T. Seki, A. Tohnai, T. Tamaki, and A. Kaito, *Macromolecules*, **29**, 4813 (1996).
67 B. Cabane, K. Lindell, S. Engström, and B. Lindman, *Macromolecules*, **29**, 3188 (1996).
68 B. Nystrom, H. Walderhaug, F. K. Hansen, and B. Lindman, *Langmuir*, **11**, 750 (1995).
69 B. Nystrom, A. L. Kjonisken, and B. Lindman, *Langmuir*, **12**, 3233 (1996).
70 G. Wang, K. Lindell, and G. Olofsson, *Macromolecules*, **30**, 105 (1997).
71 F. Tanaka, *Macromolecules*, **31**, 384 (1998).
72 F. H. Stillinger and A. Ben-Naim, *J. Chem. Phys.*, **74**, 2510 (1981).
73 H. Jacobson and W. H. Stochmayer, *J. Chem. Phys.*, **18**, 1600 (1950).
74 P. G. de Gennes, "Scaling Concepts in Polymer Physics," Cornell University Press (1979).
75 F. Tanaka, *Macromolecules*, **33**, 4249 (2000).
76 F. Tanaka and M. Ishida, *J. Chem. Soc., Faraday Trans.*, **91**, 2663 (1995).
77 C. Viebke, L. Piculell, and S. Nilsson, *Macromolecules*, **27**, 4160 (1994).
78 M. Berghmans, S. Thijs, M. Cornette, H. Berghmans and F. C. De Schryver, *Macromolecules*, **27**, 7669 (1994).
79 K. Buyse, H. Berghmans, M. Bosco, and S. Paoletti, *Macromolecules*, **31**, 9224 (1998).
80 P. L. Biagio and M. U. Palma, *Biophys. J.*, **60**, 508 (1991).
81 A. Tobitani and S. B. Ross-Murphy, *Macromolecules*, **30**, 4845, 4855 (1997).

Fumihiko Tanaka was born in Nara in 1947. He graduated from the Department of Physics, Faculty of Science, the University of Tokyo in 1971, and received his Dr. of Science degree from the University of Tokyo in 1976. During his doctoral course research, he studied disordered magnets such as spin glasses and random magnetic fields. After working for two years and a half at the same department as a research associate, he moved to Cavendish Laboratory, Cambridge, UK, where he worked on the ground-state degeneracy of Edwards -Anderson spin glass model in collaboration with Sir Sam Edwards. In 1981, he joined the Department of Physics, Tokyo University of Agriculture and Technology as an Associate Professor, and became a Professor in 1994. His main research interest there were topological interaction in polymers including supercoiling of circular DNA, polymeric coil-globule transition and thermoreversible gelation. From 1990 to 1991, he spent another one year in Cambridge to work on the rheological properties of transient networks. He moved to Kyoto University in 1997. His research mainly applies various theoretical ideas and techniques to a variety of different problems in polymer science in close relation to experiments.

Tsuyoshi Koga was born in Fukuoka in 1965. He graduated from the Department of Physics, Faculty of Science, Kyushu University in 1988, and received his doctoral degree from Kyushu University in 1993. He worked as a postdoctoral research fellow of the Japan Society for the Promotion of Science for Japanese Junior Scientists at the above Department in 1993. In 1994 he joined Hashimoto Polymer Phasing Project, ERATO, JST as a researcher. Since 1998 he has been a research associate at Department of Polymer Chemistry, Graduated School of Engineering, Kyoto University. His current research interest covers equilibrium and non-equilibrium statistical properties of complex fluids, especially associating polymers.